Individual Human Climate Analysis Applying the New Clothing Resistance Model

Ferenc Ács * and Erzsébet Kristóf

Posted Date: 5 June 2024

doi: 10.20944/preprints202406.0201.v1

Keywords: walking; sweating; thermal resistance of clothing; evaporative resistance of clothing; hu-man comfort; operative temperature; low land region of Hungary

 doi:10.20944/preprints202406.0201.v1

Article

Individual Human Climate Analysis Applying the New Clothing Resistance Model

Ferenc Ács * and Erzsébet Kristóf

Department of Meteorology, Faculty of Science, Institute of Geography and Earth Sciences, Eötvös Loránd University, Budapest, Hungary

* Correspondence: acs@caesar.elte.hu; Tel.: +36302929408

Abstract: A new clothing resistance model is described and applied to characterize the human thermal and moisture climates. The climate was described by the thermal ($r_{cl,t}$) and evaporative ($r_{cl,e}$) resistances of comfortable, imaginary clothing. The key input variable of the model is the rate of sweating (λE_{sw}). Since sweating is an individual-specific process, the model applies to the individual. The observations were carried out by a single individual in Martonvásár (Hungarian lowland, Central Europe) in the summer of 2023 and the winter of 2024. During the observations, the observer walked at a speed of 1.1-1.7 ms^{-1} in weather-appropriate clothing. Among the results, we would highlight the following: During large environmental heat surpluses, the $r_{cl,t}$ values were found to be between 0.1-0.5 clo-t (clo-t = 0.155 $m^2 \cdot °C \cdot W^{-1}$), while the $r_{cl,e}$ values fell between 0.4-0.8 clo-e (clo-e = 0.155 $m^2 \cdot hPa \cdot W^{-1}$). The values of the parameters close to 0 were caused by intense sweating (λE_{sw} > 200 Wm^{-2}). The applicability of the model is limited and largely depends on the relationship between λE_{sw} and the metabolic heat flux density.

Keywords: walking; sweating; thermal resistance of clothing; evaporative resistance of clothing; human comfort; operative temperature; low land region of Hungary

1. Introduction

The first clothing resistance models appeared in the 70s of the last century [1,2], they can be traced back to the work of Burton and Edholm [3]. Ács and co-researchers followed the philosophy of this model type, but the thermal resistance of clothing ($r_{cl,t}$) was calculated differently [4–8] with respect to the previous works [1,2,9]. We have shown that $r_{cl,t}$ is also significantly dependent on human factors [5,6,8]. In these models, the sweating term as energy balance component was not used in the energy balance equation of skin surface, so it could not be used in climates or weather situations with a large excess of heat (the value of $r_{cl,t}$ is negative in this case), when skin surface evaporation is an important component of the energy balance equation.

The above problem can only be solved if the energy balance of the skin surface is supplemented with the component of sweating. So far, we cannot simulate sweating based on the description of physiological processes. Its estimate is based on the measurement of the mass of sweat produced, this is the so-called regulatory sweating [10]. Consequently, in this new model, the rate of sweating is an input variable to be determined by measurements. Thus, the thermal resistance module of the model is supplemented with an evaporative resistance module. Both modules estimate the characteristics of comfortable clothing. Comfortable clothing is characterized by the fact that it always ensures thermal balance between the human body and its environment, and it always remains dry. Of course, this is an imaginary clothing that does not exist in real life circumstances, and due to the imposed requirements, it is suitable for characterizing the thermal and evaporative load of the climate or the weather. Since sweating is a distinctly individual-specific process, the clothing parameters characterizing the climate and weather are also individual-specific, and from this point of view, the weather and climate characterization is also individual-specific [11]. The question is to what extent deviations vary from person to person?

 doi:10.20944/preprints202406.0201.v1

The measurements and observations were carried out by a single individual. The location: Martonvásár (a small town in the Hungarian lowland, Carpathian Basin, Central Europe), period: summer 2023 and winter 2024. There was a total of 115 measurements, observations. To the best of the authors' knowledge, no similar observations and measurements for environmental, human thermal and evaporative load estimation have yet been carried out.

The goals of this study are as follows: 1) presentation of the new clothing thermal and evaporative resistance model, 2) description of the data required to run the model and description of the data collection methodology, and 3) description and analysis of the model results.

2. The Clothing Resistance Model

The model uses the energy balance equations of the clothing surface and the skin surface, it is a 1-layer clothing resistance model [12,13]. The clothing adheres closely to the human body, from below it is affected by metabolic heat flow density and water from sweating, while from above it is affected by the heat load of the environment. The change in heat and water content of the clothing was not taken into account. The clothing's parameters are: its thermal insulation capacity (resistance to heat transport), moisture insulation capacity (resistance to water vapor transport) and properties determining radiation transfer (albedo, emissivity). The former two parameters change depending on the environmental thermal load and the rate of sweating, characterizing the relationship between the individual and the weather. The radiation properties of the clothing are the input parameters of the model.

Clothing should be comfortable, that is, we should feel comfortable wearing it. This means that it must always remain dry, regardless of the rate of sweating, and we must not feel either an excess of heat or a lack of heat in it, regardless of our activity and the environmental thermal load. There is no such ideal clothing in reality, so the clothing parameters estimated with the model are the parameters of an imaginary clothing. A schematic diagram of the heat transports and state variables of the imaginary clothing is shown in Figure 1.

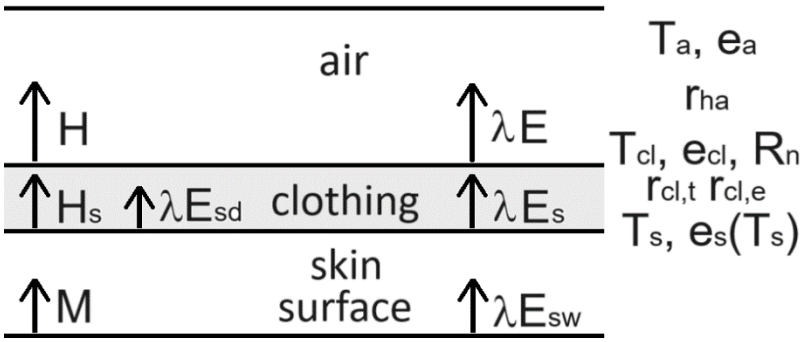

Figure 1. Heat and moisture transports and state variables that characterize imaginary clothing. H - sensible heat flux density between the clothing surface and the air, λE - latent heat flux density between the clothing surface and the air, T_a - air temperature, e_a - partial water vapor pressure of the air, T_{cl} - temperature of the clothing surface, e_{cl} - partial water vapor pressure on the clothing surface, R_n - radiation balance of the clothing surface, r_{Ha} - aerodynamic resistance to heat transport between the clothing surface and the air, H_S - sensible heat flux density between the skin surface and clothing, λE_S – latent heat flux density of skin surface evaporation, λE_{sd} – latent heat flux density of dry skin surface evaporation between the skin and clothing, λE_{sw} - the latent heat flux density of sweating, T_S - the temperature of the skin surface (34 °C), $e_S(T_S)$ - the water vapor pressure at saturation at T_S temperature, $r_{cl,t}$ - the thermal resistance of the clothing, $r_{cl,e}$ - the evaporative resistance of the clothing and M - metabolic heat flux density.

 doi:10.20944/preprints202406.0201.v1

2.1. Basic Equations

The environmental heat surplus or heat deficit strongly depends on the radiation conditions, so the radiation balance of the clothing surface is also a determining environmental factor. The two energy balances and the radiation balance can be written as follows:

$$M - H_S - \lambda E_S - W = 0, \quad (1)$$

$$R_n - H_{res} - \lambda E_{res} - H - \lambda E + H_S + \lambda E_S = 0, \quad (2)$$

$$R_n = R_{ni} - 4 \cdot \varepsilon_c \cdot \sigma \cdot T_a^3 \cdot (T_{cl} - T_a), \quad (3a)$$

$$R_{ni} = S \cdot (1 - \alpha_c) - (\varepsilon_c - \varepsilon_a) \cdot \sigma \cdot T_a^4, \quad (3b)$$

where M is the metabolic heat flux density, W is the flux density of the work of the muscles used during the activity [2], H_{res} is the respiration sensible heat flux density, λE_{res} is the respiration latent heat flux density, R_{ni} is the net isothermal radiation energy flux density on the surface of the clothing, S is the solar radiation energy flux density, α_c is the albedo of the clothing, ε_c is the emissivity of the clothing, ε_a is the emissivity of the troposphere and σ is the Stefan-Boltzmann constant. M is parameterized according to [14]. Its parameterization is described in detail in the work of Kristóf et al. [8].

2.2. Parameterizations

The following parametrizations were used to describe the heat transports in the model:

$$H_S = \rho \cdot c_p \cdot \frac{T_S - T_{cl}}{r_{cl,t}}, \quad (4)$$

$$H = \rho \cdot c_p \cdot \frac{T_{cl} - T_a}{r_{Ha}}, \quad (5)$$

$$\lambda E_S = \frac{\rho \cdot c_p}{\gamma} \cdot \frac{e_S(T_S) - e_{cl}}{r_{cl,e}}, \quad (6)$$

$$\lambda E_S = \lambda E_{sd} + \lambda E_{sw}, \quad (6a)$$

$$\lambda E_{sd} = 3{,}05 \cdot 10^{-3} \cdot (256 \cdot T_S - 3373 - e_a), \quad (6b)$$

$$\lambda E_{sw} = \frac{1}{A_f} \cdot \lambda \cdot \frac{dm}{dt}, \quad (6c)$$

$$\lambda E = \frac{\rho \cdot c_p}{\gamma} \cdot \frac{e_{cl} - e_a}{r_{Ha}}, \quad (7)$$

$$\lambda E_S = \lambda E, \quad (8)$$

Skin surface evaporation (6a) is the sum of evaporation from dry skin and skin covered in sweat. In the dry skin evaporation formula (6b), T_S is given in °C (34 °C), while e_a is given in Pa [15]. The rate of sweating (6c) cannot be simulated based on the description of physiological processes. There is a simple estimate, which is (6c), in which A_f is the surface of the human body, λ is the latent heat of evaporation and dm/dt is the loss of body weight caused by sweating, i.e. the amount of water sweated out per unit of time. This can easily be determined from the body mass and time values measured before and after the activity. The literature calls this λE_{sw} "regulatory sweating". The application of (6c) is challenging, but in our opinion it is the only reliable method for estimating the rate of sweating. The basic assumption of the model is that eq. (8) is valid. This is the guarantee that the clothing remains dry (there is neither convergence (clothing gets wet) nor divergence (clothing dries)), because we only feel comfortable in dry clothing. This makes sense, because wet clothing would sooner or later become uncomfortable due to its cooling effect. A_f was calculated by using the formula of Dubois and Dubois [16].

 doi:10.20944/preprints202406.0201.v1

2.3. The Clothing Evaporative Resistance Model

The two essential output variables of the clothing evaporation model are e_{cl} and $r_{cl,e}$. By combining (6a), (7) and (8), it is easy to express e_{cl},

$$e_{cl} = e_a + (\lambda E_{sd} + \lambda E_{sw}) \cdot \frac{\gamma}{\rho c_p} \cdot r_{Ha}, \quad (9)$$

and since both λE_{sd} and λE_{sw} can easily be estimated based on the input meteorological and human (body mass, body length) variables, e_{cl} can be calculated with ease. It can also be seen that by applying (6), (7), (8) and (9), $r_{cl,e}$ can also be expressed as follows:

$$r_{cl,e} = \frac{\rho c_p}{\gamma} \cdot \frac{e_S(T_S) - e_a}{\lambda E_{sd} + \lambda E_{sw}} - r_{Ha}, \quad (10)$$

The parametrization of r_{Ha} has already been described in several works [5,8]. The unit of $r_{cl,e}$ is [s·m^{-1}], but in the literature there is also the [clo] unit for water vapor transport. 1 clo-e = 0.155 m^2·hPa·W^{-1}, based on which 1 clo-e = 0.155·($\varrho \cdot c_p/\gamma$) = 0.155·(1.2·1004/0.65) = 287.3 s·m^{-1}.

2.4. The Clothing Thermal Resistance Model

The output variables of the clothing thermal resistance model are T_{cl} and $r_{cl,t}$. Let's express them! H_S can be expressed from (1) and described as

$$H_S = M - \lambda E_S - W = Hu. \quad (11)$$

Here, the difference in human heat flux densities is denoted by Hu. By combining (2), (5), (8) and (11), we can write the following equation:

$$R_n - H_{res} - \lambda E_{res} - \rho c_p \cdot \frac{T_{cl} - T_a}{r_{Ha}} + Hu = 0. \quad (12)$$

The final form of T_{cl} after substituting (3a) into (12) is:

$$T_{cl} = T_a + \frac{R_{ni} - H_{res} - \lambda E_{res} + Hu}{\frac{\rho c_p}{r_{Ha}} + 4 \cdot \epsilon_c \cdot \sigma T_a^3}. \quad (13)$$

Note that when estimating T_{cl}, we used both (1) (energy balance of skin surface under clothing) and (2) (energy balance of clothing surface), i.e., the magnitude of this temperature is influenced by both environmental and human factors. By combining (4) and (11), $r_{cl,t}$ can be expressed,

$$r_{cl,t} = \rho \cdot c_p \cdot \frac{T_S - T_{cl}}{Hu}. \quad (14)$$

Equations (13) and (14) are new equations and characterize the thermal properties of the clothing that creates thermal balance (neither excess of heat nor lack of heat) between the human body and its environment. Since it is clothing that creates heat balance, this clothing is imaginary. The unit of $r_{cl,t}$ is [s·m^{-1}], but the [clo] unit is also used for heat transfer. 1 clo-t = 0.155 m^2·°C·W^{-1}, based on which 1 clo-t = 0.155·($\varrho \cdot c_p$) =0.155·(1.2·1004) = 186.7 s·m^{-1}.

2.5. Operative Temperature Model

The operative temperature is a known heat load indicator. It is estimated as follows:

$$T_o = T_a + \frac{R_n}{\rho \cdot c_p} \cdot r_{Ha}. \quad (15)$$

As we can see, it depends on environmental factors (air temperature, radiation and wind). Its dependence on human factors is negligible (it is hidden in the parameterization of r_{Ha}).

 doi:10.20944/preprints202406.0201.v1

3. Location of Measurements and Observations, Tools Used

The location of the observations: Martonvásár, on the vineyard road starting next to the family house of the first author. This location made it possible to minimize the difference between the two times of weight measurement and the duration of the walk. The town Martonvásár is presented in Figure 2 on a topographical map of Hungary.

Figure 2. Martonvásár (47.31° N, 18.79° E), the location of the observations and topographical map of Hungary (Central Europe).

The body mass was measured using an Orion digital weight meter, accuracy: 0.1 kg. When the mass values were read, the time was also recorded, to the minute. We estimated the duration of walking with two devices: an AppleWatch smartwatch and a JUNSO stopwatch, this was done for control purposes. Knowing the length of the road and the duration of the walk, it was also possible to estimate the average walking speed.

4. Data

Human and weather data were used.

4.1. Human Data

Human data provide information on 1) human state variables, 2) body mass immediately before and after walking, 3) the times of body mass measurements and thus the duration of observation, and 4) the duration of walking. The following human state variables are used: body mass (most important), body length, sex, age. These data of the observer are presented in Table 1.

Table 1. Human state variables and basal metabolic heat flux density of the person conducting observations.

Person	Sex	Age [years]	Body mass [kg]	Body length [cm]	Basal metabolic heat flux density [Wm^{-2}]
the observer	male	68	89.0	190	40.8

The observer was always on foot. Walking speeds varied between 1.1 and 1.7 ms^{-1}.

 doi:10.20944/preprints202406.0201.v1

4.2. Weather Data

The weather elements used to drive the model are: air temperature, air humidity, average wind speed, wind gust speed, cloud cover and relative sunshine duration. With the exception of the last two, all data were taken from the HungaroMet (Hungarian Meteorological Service Nonprofit Zrt.) website (https://www.met.hu/en/idojaras/aktualis_idojaras/megfigyeles/) and transcribed into the database. The beeline distance between the HungaroMet automatic station and the location of the observations is less than 3 km. These data are 10-minute averages. The values of cloud cover and relative sunshine duration were estimated by the observer for the selected 10-minute time interval. Cloudiness is estimated visually in tenths. Global radiation is an hourly value expressed in Wm^{-2} (Mihailović and Ács, 1985 [17]) and refers to the hour interval in which the 10-minute observation took place. We performed a total of 115 observations in the period June 2, 2023 – March 9, 2024. The wheater elements observed ranged as follows: solar radiation varied between 0-870 Wm^{-2}, air temperature between -1-36 °C, average wind speed between 0.3-7.5 ms^{-1}, relative humidity between 34-100% and cloud cover between 0-1.

All the human data measured and weather data observed are pooled together in Table S1 of the Supplementary Material.

5. Results

Several results are presented and discussed. Since skin surface evaporation is a determining input variable, we analyzed its relationship with the rate of sweating, operative temperature and metabolic heat flux density. After that, we turned to analyzing the relationship between a) $r_{cl,t}$ and λE_s, b) $r_{cl,t}$ and T_{cl}, c) $r_{cl,e}$ and λE_s and finally d) T_{cl} and T_o. It should be mentioned that the most important output variables of the model were listed for all 115 cases, they can be viewed in Table S2 of the Supplementary material.

5.1. Sweating Rate and Skin Surface Evaporation: Dependence on M and T_o

We could see that skin surface evaporation is the sum of evaporation from dry skin and skin covered in sweat (eq. 6a). Our measurements and calculations provide insight into the relationship between these variables in the case of a walking individual. The average walking speed of the observer varied between 1.1 and 1.7 ms^{-1}. In this speed interval, the measured sweat rates varied between 0-0.8 kg/(30-45 minutes). The largest amount of water sweated out was 0.8 kg, in this case the rate of sweating was 0.8/(72 minutes). The latent heat flux density of sweating varied from 0 to 340 Wm^{-2}. In contrast, latent heat flux of evaporation from dry skin is 10-15 Wm^{-2}. λE_{sw} is the dominant component of λE_s, which can be seen in Figure 3.

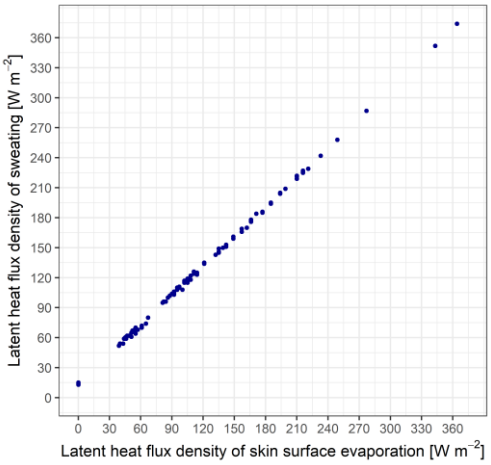

Figure 3. The relationship between the latent heat flux density of skin surface evaporation and the latent heat flux density of sweating for a walking person. Average walking speed varied between 1.1 and 1.7 ms^{-1}. The sweating rate depends on both human (for instance, M) and environmental (for

Preprints.org (www.preprints.org) | NOT PEER-REVIEWED | Posted: 5 June 2024 doi:10.20944/preprints202406.0201.v1

instance, T_o, which provides information on the integrated thermal load of the environment) factors. The point clouds characterizing the relationship between λE_S and T_o and λE_S and M can be seen in Figures 4 and 5, respectively.

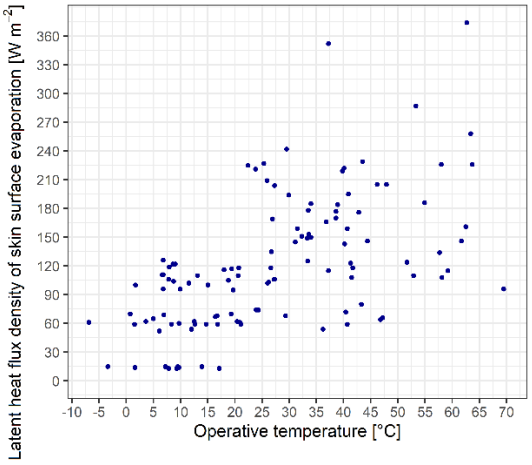

Figure 4. Scatterplot of the relationship between skin surface evaporation and operative temperature in the case of a walking observer. Observation period: June 2, 2023 -- March 9, 2024.

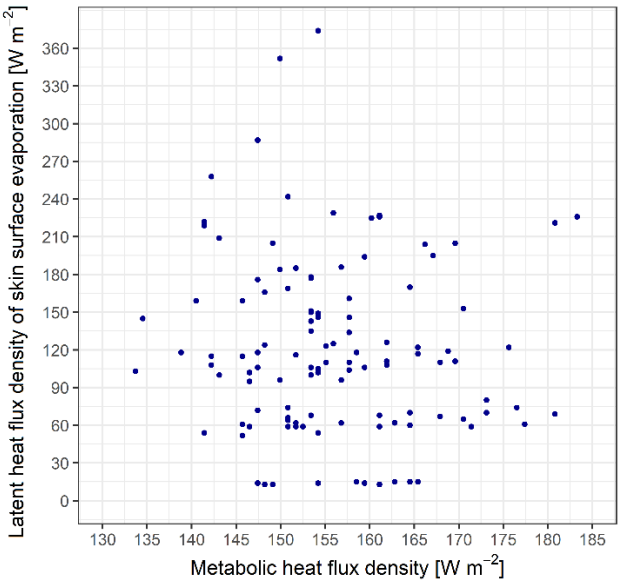

Figure 5. Scatterplot of the relationship between skin surface evaporation and metabolic heat flux density in the case of a walking observer. Average walking speed interval: 1.1-1.7 ms^{-1}, observation period: June 2, 2023 -- March 9, 2024.

We can see that the λE_S – T_o relationship emerges more distinctively than the λE_S – M relationship, but it should be emphasized that T_o varied within much wider limits (-7 – 70 °C) than M (133-183 Wm^{-2}). The large spread of points suggests that the variability of λE_S is influenced by many different and independent factors.

5.2. The Relationship between Clothing Thermal Resistance and Skin Surface Evaporation

The scatterplot of the relationship between the thermal resistance of clothing and the latent heat flux density of skin surface evaporation is presented in Figure 6.

Preprints.org (www.preprints.org) | NOT PEER-REVIEWED | Posted: 5 June 2024 doi:10.20944/preprints202406.0201.v1

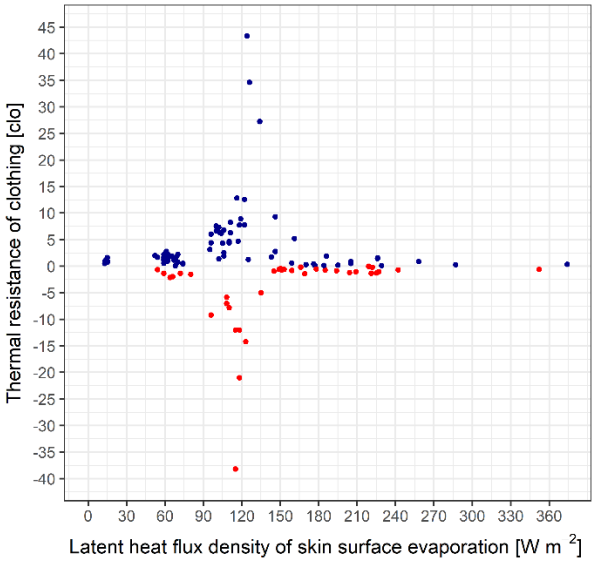

Figure 6. Scatterplot of the relationship between the clothing thermal resistance and skin surface evaporation. Blue points: the method is applicable ($r_{cl,t} > 0$), red points: the method is unapplicable ($r_{cl,t} < 0$). .

λE_S varied between wide limits (0-360 Wm^{-2}), the obtained $r_{cl,t}$ value range was 0-43 clo-t. $r_{cl,t}$ strongly depends on λE_S. It can be noticed that $r_{cl,t}$ is close to 0 for very low ($\lambda E_S < 70$ Wm^{-2}) and very high ($\lambda E_S > 165$ Wm^{-2}) λE_S values. In the range $70 < \lambda E_S < 165$ Wm^{-2}, the $r_{cl,t}$ values are greater than 3 clo-t in the vast majority of cases. It can also be noticed that in this range the value $\lambda E_S = 120$ Wm^{-2} (in this case the rate of sweating is 0.2 kg/(35 minutes)) is the limiting value, separating the increasing and decreasing $r_{cl,t}$ values. It should be emphasized that these high $r_{cl,t}$ values are not physically based, but rather the consequence of the singularity of the method (eqs. (14) and (11)). Very high $r_{cl,t}$ values occur when Hu is close to 0. It is obvious that if Hu is close to 0 and greater than zero, then $T_S > T_{cl}$ (cases of environmental heat deficit), and conversely, if Hu is close to 0, but less than zero, then $T_S < T_{cl}$ (cases of environmental heat excess). The point Hu = 0 is the singularity point of the methodology (eq. (14)).

In the case of ambient heat deficit, $r_{cl,t}$ increases with increasing λE_S. In this case, the smallest $r_{cl,t}$ values are for $\lambda E_S = 0$. These values were between 0.5 and 1.6 clo-t and, given the lack of heat, should be considered as physically based values. Note that minimal sweating (0.1 kg/(30 minutes)) significantly increases $r_{cl,t}$ values in the case of environmental heat deficit. In these cases, $r_{cl,t}$ can reach up to 2.5 clo-t.

In the case of environmental heat excess, $r_{cl,t}$ decreases with increasing λE_S. When the rate of sweating is 0.5 kg/(30 minutes), the $r_{cl,t}$ values are below 1 clo-t, which clearly shows that sweating can create a heat balance between the environment and the human body even in weather situations with a large excess of heat. Thus, for instance, for $T_o = 43.5$ °C, when $\lambda E_S = 229$ Wm^{-2} (sweating rate 0.5 kg/(44 minutes), average walking speed 1.36 ms^{-1}) $r_{cl,t} = 0.11$ clo-t, which practically means thermal neutrality.

It's to be mentioned that in cases of thermal comfort ($r_{cl,t}$ close to 0 clo-t), the absolute value of the (T_S -- T_{cl}) difference is very small (0.8-2 °C), completely regardless of which λE_S range we are talking about.

The described results refer to the blue points in the figure, in these cases the method can be used, that is $r_{cl,t} > 0$ clo-t. In the case of the red points shown in Figure 6, the method cannot be applied because $r_{cl,t} < 0$ clo-t. We will deal with the analysis of non-applicable cases separately in Section 5.6.

 doi:10.20944/preprints202406.0201.v1

5.3. The Relationship between Thermal Resistance and Surface Temperature of Clothing

The scatterplot of the relationship between clothing thermal resistance and surface temperature is presented in Figure 7.

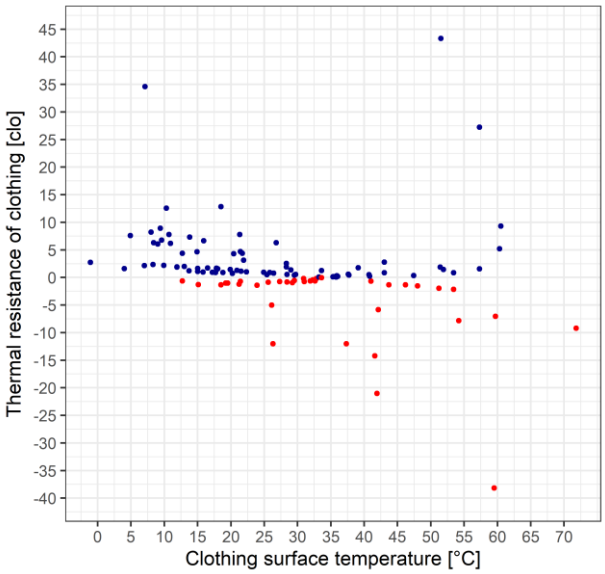

Figure 7. Scatterplot of the relationship between the clothing thermal resistance and surface temperature. Blue points: the method is applicable ($r_{cl,t} > 0$), red points: the method is unapplicable ($r_{cl,t} < 0$).

The large scatter of the points is caused by the mentioned methodological singularity (Hu → 0). Therefore, we will only look at $r_{cl,t}$ values below 4 clo-t (the $r_{cl,t}$ = 4 clo-t value can be taken as the upper limit of the heat deficit in the lowland regions of Hungary). In this case, the characteristics of the $r_{cl,t} – T_{cl}$ relationship can already be clearly recognized. The $r_{cl,t} – T_{cl}$ relationship can be divided into 3 ranges: 1) T_{cl} is much smaller than T_s, 2) T_{cl} is around T_s and 3) T_{cl} is much larger than T_s. The main characteristic of the 1st range is the lack of environmental heat, accordingly $r_{cl,t}$ gradually increases as T_{cl} decreases. This change is clearly visible. In conditions close to thermal neutrality, $r_{cl,t}$ values are by definition close to 0 clo-t. Here there is also a point with $r_{cl,t}$ = 1.3 clo-t, which is large despite the small ($T_s – T_{cl}$) difference (0.4 °C), because Hu is very small, it is only 2.2 Wm^{-2}. This result does not reflect the real thermal state, it is caused by the singularity of the methodology. In the 3rd range, there are smaller or larger excesses of heat, during which the amount of sweating can also be smaller or larger. If the excess of heat is extremely high and so is the rate of sweating, then $r_{cl,t} → 0$ clo-t. If, on the other hand, there is less sweating in such cases, T_{cl} and $r_{cl,t}$ will also be higher. If Hu becomes positive due to a small amount of sweating, then the method is unapplicable. If the environmental heat excess is smaller and the amount of sweating is also smaller, the $r_{cl,t}$ values change similarly as in the previous case. Given that we are talking about excess heat conditions, $r_{cl,t}$ values greater than 1.2-1.4 clo-t cannot be considered as physically based, but rather as caused by the singularity of the method.

5.4. The Relationship between the Clothing Evaporative Resistance and Skin Surface Evaporation

The scatterplot of the relationship between the evaporative resistance of clothing and the latent heat flux density of skin surface evaporation is presented in Figure 8.

Preprints.org (www.preprints.org) | NOT PEER-REVIEWED | Posted: 5 June 2024 doi:10.20944/preprints202406.0201.v1

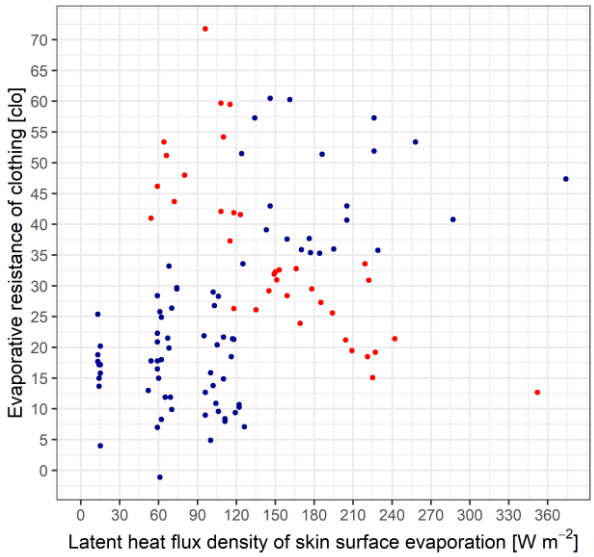

Figure 8. Scatterplot of the relationship between the clothing evaporative resistance and latent heat flux density of skin surface evaporation. Blue points: the method is applicable ($r_{cl,t} > 0$), red points: the method is unapplicable ($r_{cl,t} < 0$).

The $r_{cl,e} - \lambda E_s$ relationship is determined by the requirements (eqs. (8) and (10)) for comfortable clothing. As we can see, $r_{cl,e}$ decreases exponentially with increasing λE_s. The $r_{cl,e}$ values varied between 0.1 (for λE_s = 353 Wm^{-2}) and 21 (λE_s = 14 Wm^{-2}, there is no sweating) clo-e. If there is already sweating (λE_s = 60-80 Wm^{-2}, sweating rate is 0.1 kg/(30 minutes)), the $r_{cl,e}$ values are around 4-5 clo-e. The relationship between $r_{cl,e} - e_{cl}$ is also exponential, like the relationship between $r_{cl,e}$ and λE_s, so it is neither illustrated nor analyzed.

5.5. The Relationship between Operative Temperature and Clothing Surface Temperature

In addition to the estimation of Hu, the estimation of T_{cl} is also important for the success of the method. In the absence of direct verification, T_{cl} was compared with T_o. The scatterplot of the relationship between clothing surface temperature and operative temperature is presented in Figure 9.

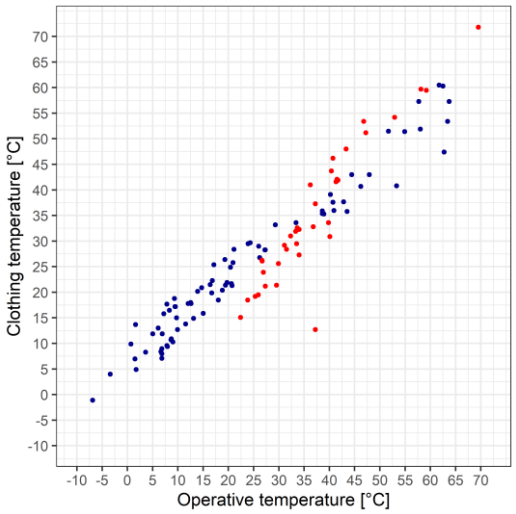

Figure 9. Scatterplot of the relationship between the clothing surface temperature and operative temperature. Blue points: the method is applicable ($r_{cl,t} > 0$), red points: the method is unapplicable ($r_{cl,t} < 0$).

Preprints.org (www.preprints.org) | NOT PEER-REVIEWED | Posted: 5 June 2024 doi:10.20944/preprints202406.0201.v1

The relationship between T_{cl} and T_o is linear, despite the scatter of points. Two ranges can be recognized: 1) in the range $T_{cl} < T_s$ the T_{cl} values are larger than the T_o values, and 2) in the range $T_{cl} > T_s$ the T_{cl} values are generally somewhat smaller than the T_o values.

5.6. Applicability of the Model

The model has limited applicability. Three cases can be distinguished: 1) the model cannot be applied because the values of $r_{cl,t} < 0$, 2) the model simulates large, non-physically based $r_{cl,t}$ values (methodological singularity) and 3) the model simulates real, physically based $r_{cl,t}$ values. All these cases can be seen in Figure 10, where the scatterplot of the $r_{cl,t}$ – Hu relationship is shown.

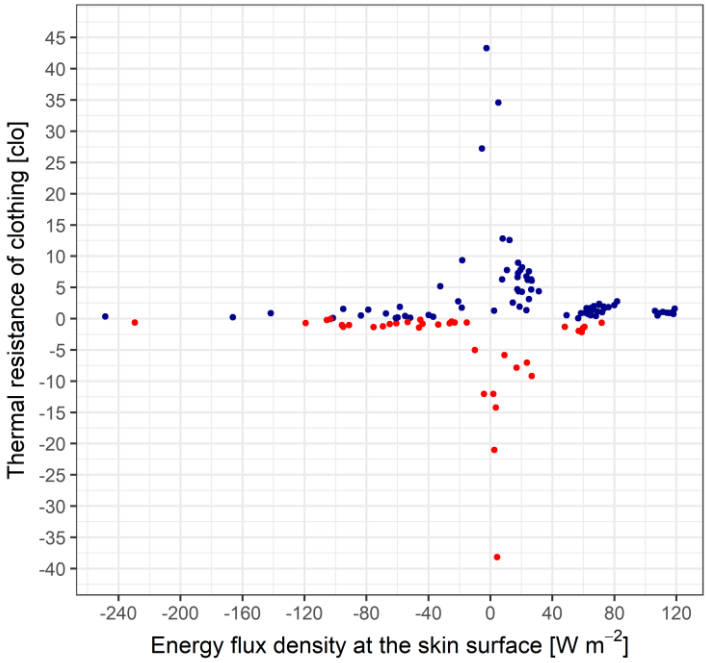

Figure 10. Scatterplot of the relationship between the clothing thermal resistance and the energy flux density at the skin surface.

Red points represent not applicable cases (case 1). The blue points with a very high $r_{cl,t}$ values (case 2) are the consequence of the methodological singularity, they are mostly in the range $-40 < Hu < 40$ Wm^{-2}. The physically based $r_{cl,t}$ values (case 3) are in the most negative (the latent heat flux density of the sweated water is much higher than the metabolic heat flux density and there is a large heat surplus) and the most positive (no sweating and there is a large heat deficit) Hu value ranges. In this figure, it is difficult to recognize the points representing the state of thermal neutrality ($r_{cl,t}$ is close to 0 clo and the temperature difference ($T_s - T_{cl}$) is small, a few °C). These cases can be seen in Figure 11 for values of T_{cl}, which are close to T_s.

Preprints.org (www.preprints.org) | NOT PEER-REVIEWED | Posted: 5 June 2024 doi:10.20944/preprints202406.0201.v1

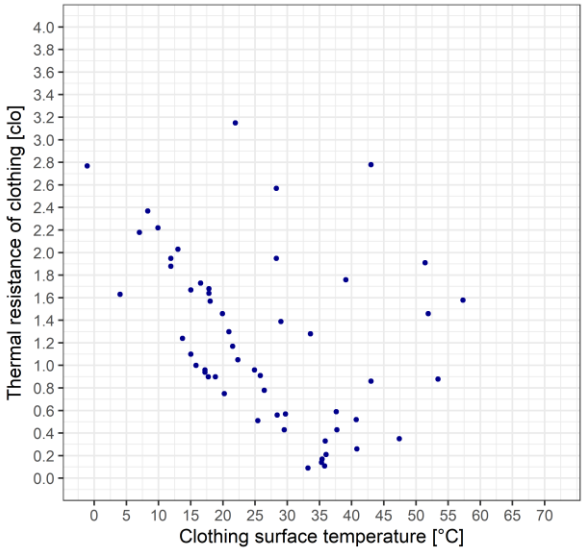

Figure 11. The scatterplot of the relationship between the clothing thermal resistance and the clothing surface temperature in the range of rcl,t < 0.8 clo.

In summary: the method performs well in the range of thermal neutrality, as well as when 1) the environmental heat surplus is high and the rate of sweating is high, 2) the environmental heat deficit is high and there is no sweating.

6. Discussion

Our measurements and analyzes showed that the model is suitable for simulating and characterizing the individual human climate. Today, there are no individual human climate descriptions, only attempts [6] that are similar to this one. The reasons for this are as follows: 1) the concept of the "standard/average" person has spread in human meteorological studies. There is no simulation for individuals, so that human variability does not have to be dealt with, and it is also important that conducting longitudinal measurements with individuals is a very tedious and complex task. 2) We characterize a human climate instead of a human thermal climate by expanding the concept of comfortable clothing. Clothing is comfortable when it is dry and thermally neutral. The imaginary clothing used in the model fulfills these two conditions. The condition of thermal neutrality was achieved by applying the energy balance equation at the clothing-air environment interface, and the condition of dry clothing is achieved by equating the latent heat flux densities leaving the skin surface and the clothing surface. Thus, the clothing was characterized not only from a thermal point of view, but also from a moisture point of view, accordingly, the model consists of a thermal and an evaporative module. With the addition of the evaporative module and its coupling to the thermal module, we obtained a new clothing resistance model.

Which are the most important results that can characterize the simulated individual human climate? We would highlight three results that refer to the environmental heat surplus, the environmental heat deficit, and thermal neutrality. In the case of high thermal loads, the $r_{cl,t}$ values were between 0.1-0.5 clo-t, while the $r_{cl,e}$ values were between 0.4-0.8 clo-e. The values of $r_{cl,t}$ and $r_{cl,e}$ close to 0 were caused by intense sweating (λE_{sw} > 200 Wm^{-2}). The former models [1,5] - as they did not simulate the process of sweating - were not applicable in these heat excess situations. In heat-deficient situations, the amount of sweating decreases, so the $r_{cl,e}$ values increase, and they are the highest when there is no sweating and the evaporation from the skin surface is equal to the evaporation from dry skin. In such cases, $r_{cl,e}$ values were around 20-21 clo-e (λE_{sd} 10-15 Wm^{-2}), $r_{cl,t}$ values varied between 0.5-1.6 clo-t. It should be mentioned that the average winter $r_{cl,t}$ values are around 1.3-1.8 clo-t [4,5] In conditions close to thermal neutrality (T_{cl} values are close to T_s), we can sweat while walking - especially if we walk at a faster pace. Thus, when $r_{cl,t}$ values were 0.1-0.4 clo-t,

 doi:10.20944/preprints202406.0201.v1

the corresponding $r_{cl,e}$ values were 0.8-3 clo-e. Sweating is considered to be natural when we walk for longer distances at higher speeds (> 1.1 ms^{-1}).

These parameters characterize imaginary clothing for an individual (Table 1). How close are the parameters of the imagined clothing to the parameters of real clothing? In this regard, we would like to make a comment about the $r_{cl,e}$ values. We observed that the t-shirt worn was always wet when sweating, this was visible. This means that the sweated water flux density is convergent, that is, the clothing absorbs water, even if the amount is negligible. Real and imaginary clothing differ in this, that is, the $r_{cl,e}$ values of the real clothing are obviously larger than the $r_{cl,e}$ values of the imaginary clothing. Therefore, the $r_{cl,e}$ values of the imagined clothing are to be considered as lower limit values.

One of the key variables in the model is the rate of sweating. λE_{sw} determines both the thermal and evaporative climate of an individual. In the cold season, λE_{sw} is minimal, close to zero; in the warm season it can be extremely high (200-300 Wm^{-2}), it depends not only on the environmental heat load, but also on the activity. In our study, the λE_{sw} – M dependence is weak (Figure 5), as M varied between narrow limits (135 – 189 Wm^{-2}), while the variability of the environmental heat load (-7 °C < T_o < 70 °C) was large. The relation of λE_{sw} to M is of decisive importance, which can be seen from equations (11) and (14) of the model. If Hu is close to 0 (there is a mathematical singularity at the point Hu = 0), the $r_{cl,t}$ values are unrealistically high, that is, they are not physically based. Little is known about the interpersonal variability of sweating [18]. To establish this, several similar longitudinal experiments would be needed, which goes beyond the framework of an individual project.

The model can be applied to all activities if M and λE_{sw} characterizing the activity are known. In our previous models, we did not estimate sweating, the activity was walking at a speed of 1.1 ms^{-1} [4–8]. Examining the applicability of the model in the case of lying down and running is one of the important goals of our future research. We can say that the model can be used in any climate, weather and activity. The determinant physiological variables of the model are M and λE_{sw}, the relationship between which is unknown in many respects.

7. Conclusions

In this study, we continued the development of the clothing resistance model type. Until now, these models [4–8] have only been used in the winter season and in cold climates, because the determination of sweating was omitted when estimating $r_{cl,t}$. We changed this concept and characterized both the thermal and moisture climates of a person by determining sweating. Since sweating is individual-specific, the model can be applied individually. Our main conclusions are as follows: 1) the human climate can be characterized not only from a thermal point of view, but also from a moisture point of view. Knowledge of sweating is necessary not only to estimate $r_{cl,e}$, but also $r_{cl,t}$. 2) Sweating is the determining variable in the estimation of both $r_{cl,t}$ and $r_{cl,e}$, but little is known about its interpersonal variability. 3) The applicability of the model strongly depends on the relationship between λE_{sw} and M, the human variability of which we know little about.

Supplementary Materials: The following supporting information can be downloaded at the website of this paper posted on Preprints.org.

Author Contributions: Conceptualization, F.Á.; methodology, F.Á.; software, F.Á. and E.K.; validation, F.Á.; formal analysis, F.Á.; investigation, F.Á.; resources, F.Á.; data curation, F.Á. and E.K.; writing—original draft preparation, F.Á.; writing—review and editing, F.Á. and E.K.; visualization, E.K.; supervision, F.Á. E.K.; project administration, F.Á.; funding acquisition, F.Á. All authors have read and agreed to the published version of the manuscript.

Funding: "This research received no external funding". Online publication cost has been funded by Publisher.

 doi:10.20944/preprints202406.0201.v1

References

1. Auliciems, A.; de Freitas, C.R. Cold Stress in Canada. A Human Climatic Classification. *Int. J. Biometeorol.* **1976**, *20*, 287–294. https://doi.org/10.1007/BF01553585.
2. Auliciems, A.; Kalma, J.D. A Climatic Classification of Human Thermal Stress in Australia. *J. Appl. Meteorol. (1962-1982)* **1979**, *18*, 616–626. https://doi.org/10.1175/1520-0450(1979)018<0616:ACCOHT>2.0.CO;2
3. Burton, A.C.; Edholm, O.G. Man in a Cold Environment. Edward Arnold Ltd., London, 1955, 273 pp..
4. Ács, F.; Zsákai, A.; Kristóf, E.; Szabó, A.I.; Breuer, H. Carpathian Basin climate according to Köppen and a clothing resistance scheme. *Theor. Appl. Climatol.* **2020**, *141*, 299–307. https://doi.org/10.1007/s00704-020-03199-z.
5. Ács, F.; Zsákai, A.; Kristóf, E.; Szabó, A.I.; Breuer, H. Human thermal climate of the Carpathian Basin. *Int. J. Climatol.* 2021, *41,* E1846–E1859. https://doi.org/10.1002/joc.6816
6. Ács, F.; Kristóf, E.; Zsákai, A. Individual local human thermal climates in the Hungarian lowland: Estimations by a simple clothing resistance-operative temperature model. *Int. J. Climatol.* 2023, *43,* 1273–1292. https://doi.org/10.1002/joc.7910
7. Ács, F.; Szalkai, Z.; Kristóf, E.; Zsákai, A. Thermal Resistance of Clothing in Human Biometeorological Models. *Geogr Pannonica* 2023, *27,* 83–90. https://doi.org/10.5937/gp27-40554
8. Kristóf, E.; Ács, F.; Zsákai, A. On the Human Thermal Load in Fog. *Meteorology* 2024, 3, 83–96. https://doi.org/10.3390/meteorology3010004
9. Yan, Y.Y.; Oliver, J.E. The Clo: A Utilitarian Unit to Measure Weather/Climate Comfort. *Int. J. Climatol.* **1996**, *16*, 1045–1056. https://doi.org/10.1002/(SICI)1097-0088(199609)16:9%3C1045::AID-JOC73%3E3.0.CO;2-O
10. Parsons, R.A., 1997: 1997 ASHRAE Handbook, Chapter 8 (Thermal Comfort), Evaporative Heat Loss from Skin, 8.3 pp.
11. Rovelli, C. Helgoland: Making Sense of the Quantum Revolution. Park Kiadó, Budapest, 2022, 269 pp. ISBN: 978-963-355-725-9. (in Hungarian)
12. Campbell, G.S.; Norman, J. An Introduction to Environmental Biophysics; 2nd edition; Springer: New York, 1997. ISBN 978-0-387-94937-6.
13. Katić, K.; Li, R.; Zeiler, W. Thermophysiological Models and Their Applications: A Review. *Build. Environ.* **2016**, *106*, 286–300. https://doi.org/10.1016/j.buildenv.2016.06.031
14. Weyand, P.G.; Smith, B.R.; Puyau, M.R.; Butte, N.F. The mass-specific energy cost of human walking is set by stature. *J. Exp. Biol.* **2010,** *213,* 3972–3979. https://doi.org/10.1242/jeb.048199
15. Fanger, P.O. Thermal comfort: analysis and applications in environmental engineering. *PhD Thesis*, Danmarks tekniske højskole, Danish Technical Press, Copenhagen, 1970, 244 pp. ISBN: 8757103410 9788757103410.
16. Dubois, D.; Dubois, E.F. The Measurement of the Surface Area of Man. *Archives of Internal Medicine* **1915**, *XV*, 868–881. https://doi.org/10.1001/archinte.1915.00070240077005.
17. Mihailović, D.T.; Ács, F. Calculation of daily amounts of global radiation in Novi Sad. *Időjárás* **1985,** *89*, 257–261. (In Hungarian)
18. *Lim, C.L.* Fundamental Concepts of Human Thermoregulation and Adaptation to Heat: A Review in the Context of Global Warming. Int. J. Environ. Res. Public Health, **2020,** *17, 7795.* https://doi.org/10.3390/ijerph17217795.